Article

Synthesis of Gold Functionalised Nanoparticles with the *Eranthis hyemalis* Lectin and Preliminary Toxicological Studies on *Caenorhabditis elegans*

Jamila Djafari [#1,2], Marie T. McConnell [#3], Hugo M. Santos[1,2], José Luis Capelo [1,2], Emilia Bertolo [3*] Simon C. Harvey [3], Carlos Lodeiro [1,2], and Javier Fernández-Lodeiro [1,2*]

[1] BIOSCOPE Group. LAQV@REQUIMTE. Chemistry Department. Faculty of Science and Technology. University NOVA of Lisbon. Caparica Campus. 2829-516 Caparica. Portugal.
[2] PROTEOMASS Scientific Society. Rua dos Inventores. Madam Parque. Caparica Campus. 2829-516 Caparica. Portugal.
[3] Biomolecular Research Group. School of Human and Life Sciences. Canterbury Christ Church University. Canterbury. Kent CT1 1QU. UK.
* Correspondence: emilia.bertolo@canterbury.ac.uk and j.lodeiro@fct.unl.pt
# These two authors have contributed equally to this work

Abstract: The lectin found in the tubers of the Winter Aconite (*Eranthis hyemalis*) plant (EHL) is a Type II Ribosome Inactivating Protein (RIP); type II RIPs have shown anti-cancer properties, and have great potential as therapeutic agents. Similarly, colloidal gold nanoparticles are successfully used in biomedical applications as gold nanoparticles can be functionalised with ligands with high affinity and specificity for target cells to create therapeutic and imaging agents. Herein we present the synthesis and characterization of gold nanoparticles conjugated with EHL. The aim was to establish the viability of the conjugate and perform a set of initial assays to establish whether the biological effect of EHL is altered by the conjugation. The biological assays were performed in *Caenorhabditis elegans*, a free living nematode commonly used for toxicological studies; previous work from some of the authors using first life stage (L1) nematodes has shown that EHL has a strong biocidal effect on *C. elegans*. Gold nanoparticles functionalised with EHL (AuNPs@EHL) were successfully synthesised by bioconjugation with citrate gold nanoparticles (AuNPs@Citrate); the conjugates were analysed by UV-Vis spectroscopy, Dynamic Light Scattering (DLS), Zeta Potential analysis and Transmission Electron Microscopy (TEM). Results indicate that an optimal functionalisation was achieved with the addition of 100 µL of EHL (concentration 1090 ± 40 µg/mL) over 5 mL of AuNPs (concentration [Au0] = 0.8 mM). Biological assays on the effect of AuNPs@EHL on *C. elegans* were performed, using first life stage (L1) and pre-adult stage (L4) nematodes. Citrate gold nanoparticles did not have any obvious effect on the nematodes. For L1

stage nematodes, the assays show that conjugation with gold nanoparticles reduced the biological effect of EHL on *C. elegans*. As lectin binding activity is essential for the natural protein to bind and allow entry to cells, conformational changes due to conjugation may have affected this binding affinity. For L4 stage nematodes, both EHL alone and AuNPs@EHL showed biological activity, and reproductive delays and reduced fecundity were observed in both cases. These assays indicate that EHL can be conjugated to gold nanoparticles and retain elements of biocidal activity.

Keywords: *Caenorhabditis elegans*; Toxicity; gold nanoparticles; nanocomposites; Lectin Protein; ROS

1. Introduction

Lectins are a class of proteins ubiquitously expressed in plants, animals, bacteria and viruses. They are well known for their ability to agglutinate erythrocytes, a property that enabled the development of the ABO system of blood typing [1]. Another characteristic common to all lectins is their ability to bind carbohydrates selectively based on the individual sugar specificity of the lectin [2]. Plant lectins play a key role in plants' defences, with many specifically binding to epithelial cells of herbivore and nematode guts [3,4]. Insecticidal, antifungal and antiviral qualities have also been widely described [5- 8]. *Eranthis hyemalis*, commonly known as Winter Aconite, is a late winter/early spring flowering perennial plant of the family Ranunculaceae. Research carried out by Cammue et al. [9] and Kumar et al. [5] indicated that the tubers of *E. hyemalis* possessed a proteinaceous toxin, found to cause agglutination of erythrocytes as well as impacting on the fitness of some formidable herbivorous agricultural pests and plant viruses. The toxin was named *Eranthis hyemalis* lectin (EHL). To date *E. hyemalis* is the sole representative of the Ranunculaceae to be reported to express lectin activity. Due to the structural and toxicity studies conducted [5, 9-11]. EHL should be more accurately described as a Type II Ribosome Inactivating Protein (RIP). RIPs are a class of enzymes (EC 3.2.2.22) with a mode of action which results in the breakage of a glycosidic bond in the 28s rRNA in the 60S subunit of the ribosome, resulting in halt of protein synthesis and subsequent cell death. EHL shows specificity for N-acetyl-galactosamine [5,9], an overexpressed and incompletely glycosylated sugar in the Tn antigen which characterizes cancer linked O-glycans [12]. Other N-acetyl-galactosamine specific RIPs such as the Mistletoe lectin and Riproximin have demonstrated promising therapeutic relevance as anticancer agents [13-15]. EHL could thus have a promising future as an anticancer agent, if its toxicity can be harnessed and tuned to appropriate levels.

Previous work by some of the authors has shown biocidal effects of EHL against the free living nematode *Caenorhabditis elegans* [16]. *C. elegans* is a well-established model organism for initial toxicological studies due to the conserved nature of its biological and biochemical processes, including the stress response and disease pathways [17]. A wide range of mutant phenotypes available, short life cycle of the worms, well documented reproductive and lifespan schedule, and their largely transparent body type (which makes it possible to observe unusual effects easily), are some of the advantages of *C. elegans* [18]. Developing *C. elegans* individuals pass through a well-defined set of life stages, with individuals hatching as first larval stage (L1) worms. These L1 worms subsequently molt through three further larval stages – the L2, L3 and L4 stages - before maturing as adults. Development is temperature dependent and takes approximately 3 days at 20°C. Newly hatched L1 worms measure around 0.25mm in length, and in their adult stage they reach up to 1mm. An interesting characteristic of *C. elegans* is its ability to enter an alternate L3 life cycle stage known as the dauer larvae. Naturally induced dauer larval arrest occurs when L1 and L2 larva are

 doi:10.20944/preprints201805.0141.v1

exposed to environments not suited for growth and reproduction [19]. These environments are characterised by a depleted food source and population overcrowding, with the chemosensory cues and signals for these detected by the L1 larvae. As part of development into dauer larvae, worms develop a specialized outer cuticle, and seal their mouths preventing feeding. In combination with changes in their metabolism, these adaptations mean that dauer larvae have an increased lifespan, an enhanced resistance to environmental stress and are resistant to many chemical treatments that would kill other lifecycle stages. This resulting dauer larvae is in an arrested developmental state (a temporary halt in its development), and can survive for months until conditions improve, at which point development resumes with dauer larvae moulting in to L4s [19].

Colloidal gold nanoparticles (AuNPs) have long been exploited in science for their optical properties. Localized surface plasmon resonance (LSPR) is the oscillation of charge density in metallic particles when subjected to excitation [20]. The SPR of a nanoparticle can be excited at a specific frequency of light depending on the size, shape, and surface topography of a particle, resulting in strong and characteristic light scattering and intense energy absorption; this property used in tumour destruction through the technique of photothermal ablation [21]. The applications of AuNPs have increased enormously in recent years and are used routinely in both material science and within biomedical sciences as therapeutic agents and drug delivery vehicles [22,23]. AuNPs have inherently low toxicity and biological compatibility, and the ability to be conjugated to a variety of useful substrates such as peptides and therapeutic drugs [20]. AuNPs can be functionalized with both therapeutic and imaging agents simultaneously, thus are a powerful tool in cellular studies [24]. Gold nanoparticles can be functionalized with ligands with high affinity and specificity for target cells such as the Tn antigen, which is where conjugating gold nanoparticles with a RIP such as EHL presents an opportunity to fine tune EHL's biological effects.

Herein we present the synthesis and characterization of AuNPs conjugated with EHL (AuNPs@EHL), and the preliminary study of the effects of AuNPs@EHL on *C. Elegans*. The aim was to establish the viability of the conjugate and perform a set of initial assays to establish if the biological effect of EHL is altered by the conjugation. The conjugates were analysed by UV-Vis spectroscopy, Dynamic Light Scattering (DLS), Zeta Potential analysis and Transmission Electron Microscopy (TEM). Biological assays on the effect of AuNPs@EHL on *C. elegans* were performed using first life stage (L1) and pre-adult stage (L4) nematodes, and the results compared to previously published data on the effect of EHL on L1 nematodes [16]. Additionally, the effects of naked AuNPs on L1 and L4 nematodes, and the effect of EHL on L4s were also studied.

2. Materials and methods

2.1. Materials

Tetrachloroauric (III) acid ($HAuCl_4.3H_2O$), Sodium hydroxide (NaOH), Hydrochloric acid (HCl), Sodium chloride (NaCl) and Sodium citrate tribasic ($C_6H_5Na_3O_7.2H_2O$) have been purchased from Sigma Aldrich, Strem Chemicals, Fluka or Panreac, and used without further purifications. Acetonitrile (CAN, 99.9% purity) and acetic acid glacial (99.7% purity) were purchased from Sigma-Aldrich. Ethanol (EtOH, 96% purity) was purchased in Panreac. Water was always Milli-Q grade by Millipore.

Protein quantification was accomplished by measuring the absorbance at 280 nm with the use of a NanoDrop 1000 Spectrophotometer from Thermo Scientific. Gold nanoparticles were characterized by UV-Vis spectrophotometer Jasco V-630 and Jasco V-650 UV-Vis (Easton, MD, UK from the Proteomass-BIOSCOPE Facility lab). The transmission electron microscopy (TEM) images were obtained using a JEOL JEM 1010F transmission electron microscope from the CACTI, University of Vigo, (Spain), operating at 100 kV. Samples were prepared dropping 5 µL of the colloidal suspension on a copper grid coated with a continuous carbon film, and the solvent was

 doi:10.20944/preprints201805.0141.v1

allowed to evaporate. TEM Images were characterized using Image J software. Histogram was prepared counting a minimal of three hundred nanoparticles. The size measurements were performed with the nanoparticles diluted in 1 mL of water in a Zetasizer Nano ZS instrument (Malvern Instruments) in the PROTEOMASS facilities. Zeta potential quantification was carried out in the same Zetasizer Nano ZS instrument.

2.2. Synthesis of EHL conjugated gold nanoparticles (AuNPs@EHL)

The AuNPs@Citrate were prepared by modification of a previously published protocol [25]. An aqueous solution (125 mL) containing 49 mg of tetrachloroauric (III) acid ($HAuCl_4.3H_2O$) was heated until boiling point without reflux to ensure a low temperature gradient in the walls of the flask; the solution was kept boiling for 10 minutes. Then, a pre-boiled aqueous solution (12.5 mL) containing 147 mg of sodium citrate tribasic ($C_6H_5Na_3O_7.2H_2O$) was added rapidly. The reaction mixture was heated to boiling for an additional 15 min, and then allowed to cool to ~25 °C and left with magnetic stirring overnight. The reaction was then diluted to a final volume of 140 mL with milliQ water and was transferred into a glass bottle for storage. The final obtained citrate gold nanoparticles (AuNPs@Citrate) presented a concentration of 0.8 mM in terms of Au (0) (See SI for details) and were used without purification.

To achieve the bioconjugation of the AuNPs@Citrate with EHL, the protein was suspended in PBS solution. Quantification via Bradford technique indicated an EHL concentration of 1090 ± 40 µg/mL. Six experiments were performed in order to characterize the optimal quantity of EHL to achieve the stabilization of the nanoparticles: 25 µL, 50 µL, 100 µL, 200 µL, 300 µL and 500 µL of EHL solution were used. On each case, the EHL solution was added onto 5 mL of AuNPs@Citrate ([Au(0)] = 0.8 mM) and left under vigorous stirring at room temperature for 2h, to ensure effective functionalization. The nanoparticles obtained AuNPs@EHL-1 (25 µL), AuNPs@EHL-2 (50 µL), AuNPs@EHL-3 (100 µL), AuNPs@EHL-4 (200 µL), AuNPs@EHL-5 (300 µL), AuNPs@EHL-6 (500 µL), were isolated by centrifugation at 14000 rpm during 25 min, and then suspended in PBS solution. A second centrifugation cycle and resuspension in 5 mL of MilliQ water were performed. The first supernatant was filtered in a cellulose filter of 0.22 µm, and quantified by the Bradford technique, in order to determine EHL concentration at the nanoparticles surface. AuNPs@EHL-3 (100 µL) was selected to perform the biological studies (See Figure 3S in the Supplementary Information, SI)

3.2 Nematode assay

Worms were obtained from the *Caenorhabditis* Genetics Center and maintained using standard methods [26] on nematode growth media plates (NGM) using an *Escherichia coli* OP50 strain food source. *C. elegans* strain N2 was used for the assays. In all experiments, treatments and genotypes were blind coded, the position of plates within experimental blocks was randomised, and any contaminated plates displaying evidence of fungal growth were excluded from all analysis. Assays were initiated using arrested and synchronised *C. elegans* first stage larvae (L1s) obtained by allowing eggs, isolated from gravid hermaphrodites by hypochlorite treatment [26], to hatch on NGM plates in the absence of food for 24 hours at 20°C.

For the experiments on L1 stage worms, synchronised L1s were incubated in 15 ml eppendorf tubes at 20ºC in a solution of one of four treatments (see below) for 6 hours. 3 replicates of each treatment were made. After incubation, all treatments were subjected to a cycle of 3 washes with M9 buffer [26] with a 2 minute centrifugal spin at 2000G. Worms were then added to seeded (*Escherichia coli* OP50) NGM plates and incubated at 20ºC. Plates were then scored on day 3 for survival, arrested development and for dauer larvae formation.

For the experiments on L4 stage worms, synchronised L1s were placed on seeded NGM plates and incubated at 20ºC until the L4 stage was reached. Treatment was then carried out in the same

Preprints (www.preprints.org) | NOT PEER-REVIEWED | Posted: 9 May 2018 doi:10.20944/preprints201805.0141.v1

set of liquid conditions as experiment 1 for 18 hours, with tubes placed in a shaking incubator at 20ºC overnight. As previously, worms were then washed 3 times and moved onto *en masse* onto NGM plates (one plate per tube). L4 stage worms were then individually picked from these plates onto seeded NGM plates, 50 per treatment. Worms were then transferred to new plates daily during the reproductive period, with progeny allowed to develop for 2 days before they were counted. Treatments were as follows: First, M9 liquid nutrient media and EHL @ [1.51 mg/ml]; second, M9 liquid nutrient media and AuNPs@EHL-3; third, M9 liquid nutrient media and AuNPs@EHL and fourth, M9 liquid nutrient media.

3. Results and Discussion

3.1. Synthesis and Characterization of the bioconjugated gold nanoparticles (AuNPs@EHL)

AuNPs@EHL were synthesized by attaching the protein to the nanoparticles surface through adsorption. This methodology has been widely adopted to prepare many nanoparticles/protein bioconjugates [26- 30]. In our case, the bioconjugation was achieved by incubating the AuNPs@Citrate in water solution, with an EHL solution in phosphate-buffered saline (PBS). The particles were analyzed by UV-Vis spectroscopy, DLS, Zeta Potential and TEM analysis. The ruby red colloidal solution of AuNPs@Citrate presents a Localized Surface Plasmon Resonance (LSPR) band at 519 nm in the UV-Vis spectrum. TEM analysis shows that the spherical AuNPs@Citrate have an average size 14.4 nm (SD = 1.13) (see Figure 1). DLS experiments indicated that the AuNPs@Citrate measured 18.80 nm in Z-average, with a Zeta Potential equal to -43.6 mV/cm, confirming the nanoparticles stabilization by citrate molecules. The concentration of the gold colloid obtained, in terms of Au(0), has been calculated from the absorption at 400 nm [32, 31-33]. Thus we have obtained a concentration of [Au(0)] = 0.8 mM (see SI for details).

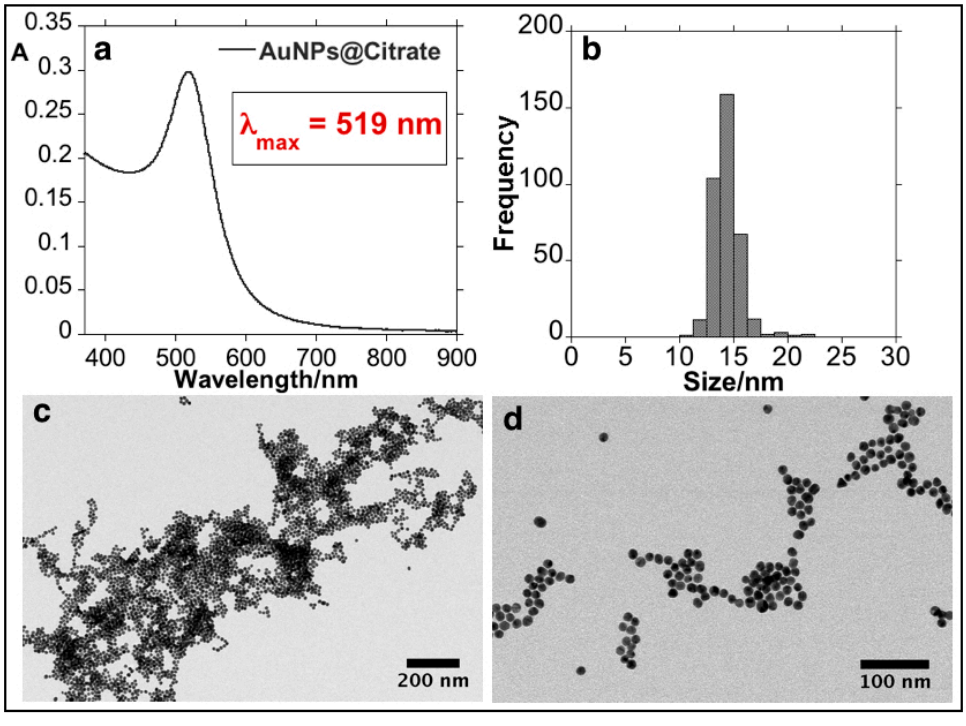

Figure 1 – UV-Vis spectrum (a) histogram (b) and low magnification TEM images (c and d) of AuNPs@Citrate. The histogram has been performed counting 300 nanoparticles using Image J software.

An incubation process was performed to conjugate the AuNPs@Citrate with EHL; the concentration of the EHL solution used (determined by the Bradford technique) was 1090 ± 40 µg/mL. Six experiments were performed in order to characterize the optimal quantity of EHL to achieve the stabilization of the nanoparticles. The following volumes of EHL solution were used: 25

 doi:10.20944/preprints201805.0141.v1

μL (AuNPs@EHL-1), 50 μL (AuNPs@EHL-2), 100 μL (AuNPs@EHL-3), 200 μL (AuNPs@EHL-4), 300 μL (AuNPs@EHL-5), and 500 μL (AuNPs@EHL-6). All the nanoparticles obtained were characterized by UV-Vis spectroscopy, DLS, Zeta Potential and TEM. Results are summarized in Table 1 and Figure 3S (see SI).

Table 1.- AuNPs@EHL solution composition for each experiment, DLS and Zeta Potential Values and protein amount on the nanoparticles ([EHL] = concentration of EHL)

AuNPs@EHL sample	**1**	**2**	**3**	**4**	**5**	**6**
Vol. EHL added (μL)	25	50	100	200	300	500
Total vol. of the reaction (μL)	5025	5050	5100	5200	5300	5500
Mass EHL in the reaction (μg)	27.3	54.5	109	218	327	545
Mass EHL in supernatant (μg/mL)	3.1±0.1	7.4±0.3	4.0±0.1	40±2	61.1±0.4	84±3
Mass EHL in VT supernatant (μg)	15.6±0.5	37.4±0.3	20.4±0.1	208.0±10	323.8±2	462.0±17
[EHL] in the NPs (μg)	11.7	17.1	88.6	10.0	3.2	83.0
Z-Average value (nm)	266.4	90.3	54.4	51.7	60.8	51.3
Polydispersity Index (PDI)	0.29	0.26	0.28	0.42	0.44	0.44
Zeta Potential (mV/cm)	-23.1	-19.8	-27.8	-24.6	-20.2	-29.4

Addition of low quantities of EHL (AuNPs@EHL-1 and AuNPs@EHL-2) does not allow the stabilization of the colloidal system, and induce nanoparticles aggregation by partial functionalization. As it can be seen in Figure 2, a red shift on the LSPR band was observed. In addition, the aggregation of the nanoparticles was confirmed by the increase in Z-average value obtained for this samples (see Figure 3 and Figure 2-SI). TEM images also confirm that aggregation has occurred (see Figure 4 (a)). Due to its dimeric structure, EHL could act as a link between the nanoparticles, and thus induce aggregation in the colloidal system. Moreover, due to the incomplete formation of the nanoparticles' corona, in the presence of PBS salts it could modify the isotropy charge produced by the citrate adsorbed in the surface, resulting in the formation of nano-aggregates.

Preprints (www.preprints.org) | NOT PEER-REVIEWED | Posted: 9 May 2018 doi:10.20944/preprints201805.0141.v1

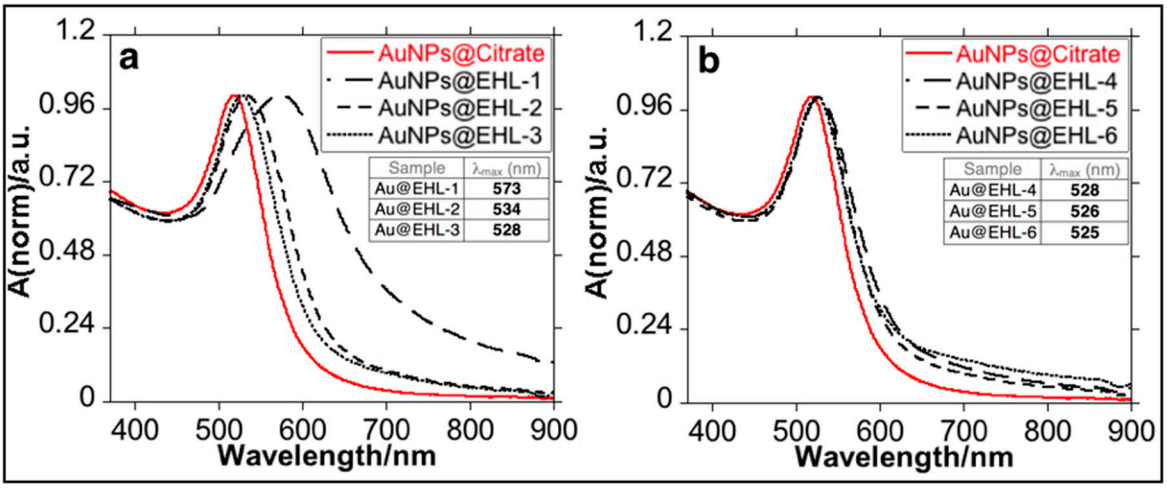

Figure 2. UV-Vis spectra of the different AuNPs@EHL samples synthesized: (**a**) AuNPs@EHL-1, AuNPs@EHL-2, and AuNPs@EHL-3; and (**b**) AuNPs@EHL-4, AuNPs@EHL-5, and AuNPs@EHL-6.

For higher amounts of EHL (AuNPs@EHL-4, AuNPs@EHL-5 and AuNPs@EHL-6), saturation of the nanoparticles surface occurs, as shown by the similar λmax of the LSRP band when compared with AuNPs@EHL-3, together with the similar Z average obtained (see Figure 3 and Figure 2S in SI). Moreover, a significant increase in PDI (polydispersity index) was observed for AuNPs@EHL-4, AuNPs@EHL-5 and AuNPs@EHL-6 (see Figure 3 and Figure 2S in SI). These results suggest that the colloidal systems conjugated in these conditions were composed of AuNPs@EHL and an excess of EHL molecules. In our case, additional centrifugation cycles were not able to wash the unreacted EHL. To this respect, the decrease in the rotational speed in the time intervals studied (between 20 min and 1 h) resulted in a considerable increase in the concentration of AuNPs in the supernatant. (See Figure 3S in SI)

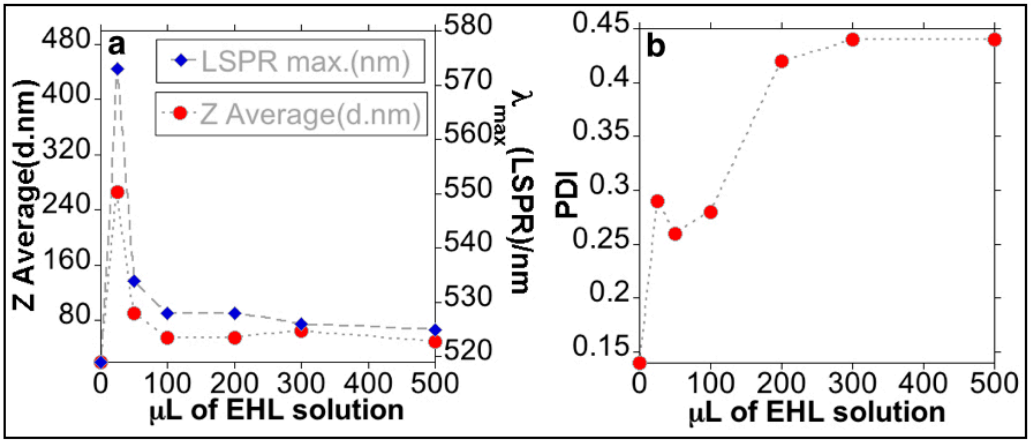

Figure 3: (**a**) Z-average (red dot) and LSPR maximum (blue dot) and (**b**) PDI (polydispersity Index) of the AuNPs@EHL obtained as a function of EHL amounts added.

In an attempt to quantify the amount of protein on the surface of NPs we have analyzed the first supernatant obtained during the purification process of the nanoparticles using the Bradford technique. For higher amounts of EHL (AuNPs@EHL-4, AuNPs@EHL-5 and AuNPs@EHL-6), this supernatant was not completely clear and still contained nanoparticles, even after filtering, which can produce an erroneous reading using the Bradford technique. This is because in spectroscopic

Preprints (www.preprints.org) | NOT PEER-REVIEWED | Posted: 9 May 2018 doi:10.20944/preprints201805.0141.v1

quantification the wavelength used may overlap with the LSPR band of the AuNPs, resulting in the appearance of increased protein values (see Table 1).

The results obtained suggest that the best functionalization is achieved with the addition of 100 µL of protein (1090 ± 40 µg/mL) onto 5 mL of AuNPs@Citrate solution. The AuNPs@EHL obtained (sample AuNPs@EHL-3) show a high percentage of protein functionalized (17.7 µg/mL); TEM images and DLS analysis confirm lack of aggregation and the stability of the resulting colloidal solution (See Figure 4 (B) and Figure 2S in SI). UV-Vis spectra show a redshift in the LSPR band from 519 nm to 528 nm (see Figure 3) suggests a composition change on the surface of the nanoparticles, indicative of the protein adsorption [34]. The Z-average increased from 18.8 nm (for AuNPs@Citrate) to 54.4 nm for AuNPs@EHL-3.

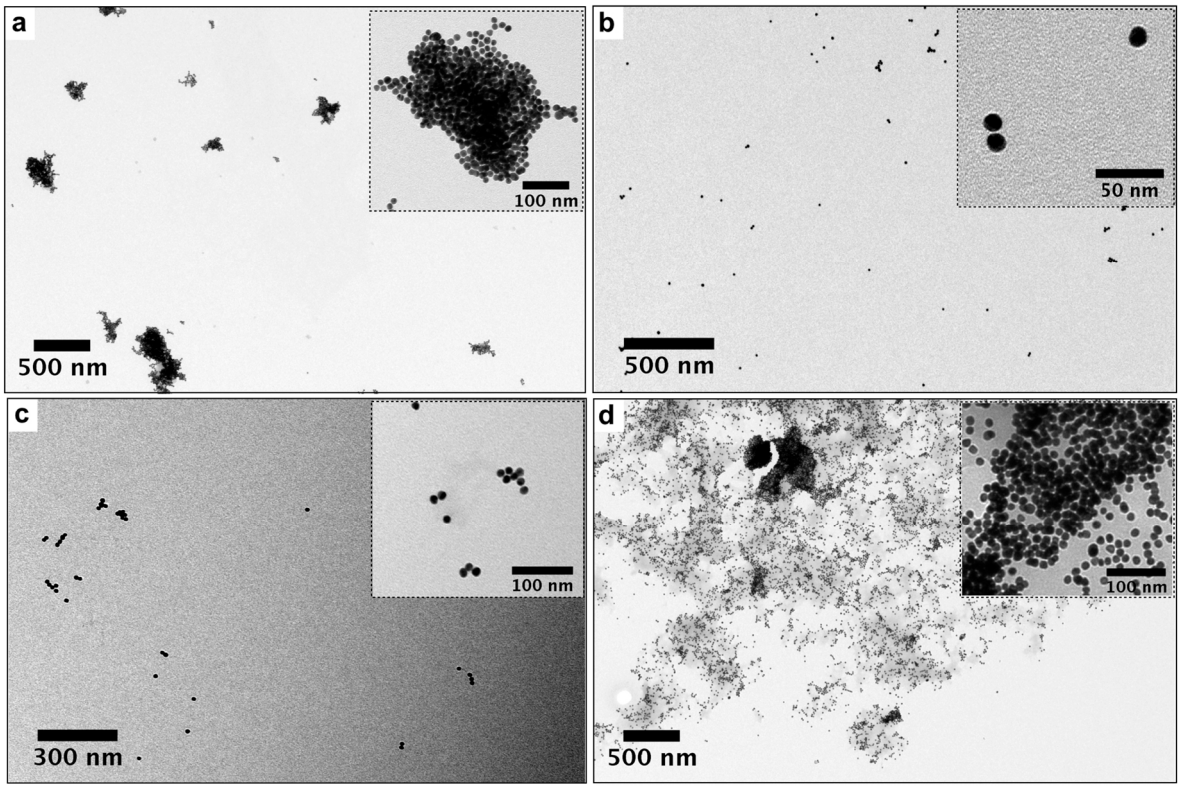

Figure 4. TEM images of AuNPs@EHL when different amounts of protein are added: **(a)** AuNPs@EHL-2 (25 µL), **(b)** AuNPs@EHL-3 (100 µL), **(c)** AuNPs@EHL-5 (200 µL) and **(d)** AuNPs@EHL-2 (500 µL). In all cases the nanoparticles go through two centrifugation cycles (14000 rpm x 25 minutes) and are resuspended in MilliQ water.

In order to show that the EHL is indeed conjugated to the surface of the nanoparticles a test was carried out by adding 200 µL of 2M NaCl to a solution of 3 mL of the respective gold colloid (factor dilution 1:10); results are shown in Figure 5. When NaCl was added to the AuNPs@Citrate, the colloid aggregation occurred. This phenomenon can be visualized through the color change of the solution from red to blue accompanied by a marked red-shift in λ_{max} of the LSRP band. Due to the presence of electrolytes such as sodium chloride, the negative charge of the colloids is masked causing an imbalance between the repulsive and attractive forces and producing colloid aggregation [35]. The addition of NaCl onto AuNPs@EHL-3 did not result in any destabilization of the system, showing that EHL molecules are on the nanoparticles surface.

Preprints (www.preprints.org) | NOT PEER-REVIEWED | Posted: 9 May 2018 doi:10.20944/preprints201805.0141.v1

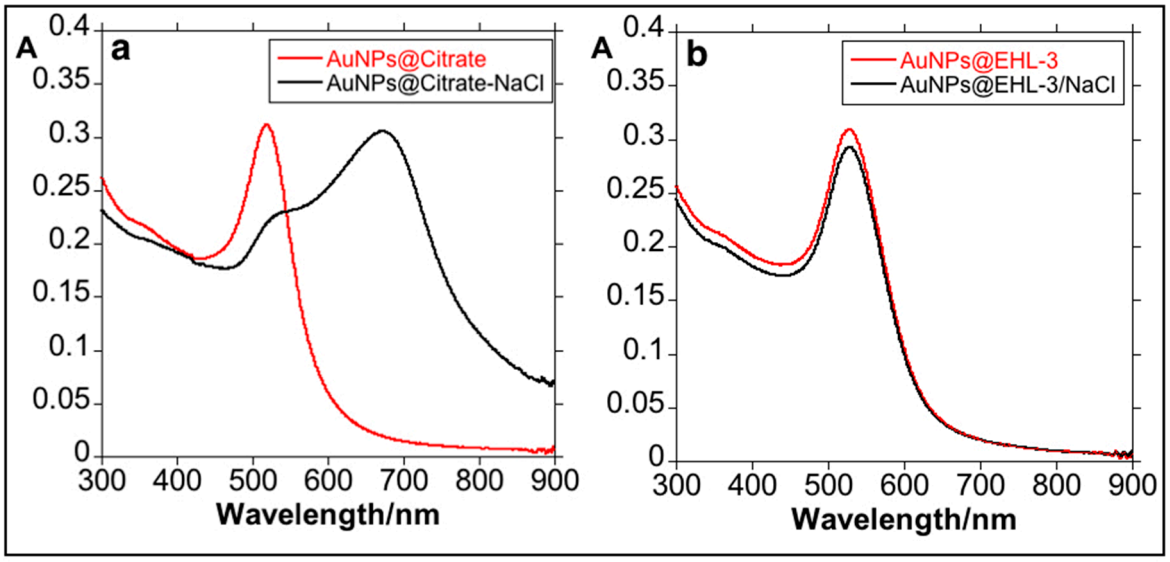

Figure 5. UV-Vis study of the effects of adding of 200 µL NaCl 2M to 3 mL of AuNPs@Citrate (left) and AuNPs@EHL-3 (right); dilution factor 1:10.

3.2 Biological activity against C. elegans

The effect of AuNPs@EHL on *C. elegans* was investigated, and compared to the effect of AuNPs@Citrate treatment and EHL treatment. The biological studies were performed using AuNPs@EHL-3 (which from now on will be referred to as AuNPs@EHL). Previous work by some of the authors has shown that EHL has biocidal properties against *C. elegans*, producing a significant reduction in fecundity, development and growth. Additionally, the authors reported a high incidence of abnormal dauer development when arrested L1 larvae were treated with EHL and then maintained on food, *i.e.* EHL treatment resulted in dauer larvae formation under conditions that produced 100% non-dauer development in non-treated worms. These EHL-induced dauer larvae were also unable to resume development when maintained on food. The authors called this a "lectin-induced effect" and suggested that the occurrence of dauer formation and a failure to recover in the presence of food indicates that EHL is binding specifically to amphid neurons [16].

Here, two sets of experiments were performed. The first set was a replication of the work on the effects of EHL on *C. elegans* [16], using AuNPs@EHL. The second set of experiments (set 2) were carried out using L4 stage (pre-adult) worms and had not previously been conducted with EHL. An observation that the AuNPs@EHL sample did not agglutinate erythrocytes; a characteristic of the native protein, was recorded prior to commencement of the experiments. This effect suggests that conjugation changes important properties in the native protein.

For the first set of experiments L1 stage worms were treated with AuNPs@Citrate, AuNPs@EHL and EHL, as well as a control group with no treatment. For the treated L1s, the expected dauer larvae and developmental arrest in response to EHL treatment was observed. However, there is no dauer larvae formation in response to AuNPs@Citrate or AuNPs@EHL, and none in the control. As previously reported, EHL also killed L1s in this assay, whilst the other treatments did not differ in L1 survival (see Table 2). From these

Preprints (www.preprints.org) | NOT PEER-REVIEWED | Posted: 9 May 2018 doi:10.20944/preprints201805.0141.v1

results, we conclude that AuNPs@Citrate do not obviously affect L1s, and that the AuNPs@EHL do not replicate the EHL effect. In conjunction with the empirical observation that agglutination properties were absent from the AuNPs@EHL sample, this would indicate that a conformational change has occurred potentially in the protein induced by conjugation to the nanoparticles, which blocks the EHL neuronal binding effects.

Table 2. EHL treatment affects survival and development of treated *C. elegans* L1s. When scored, adult worms were only observed on 3 of the 12 EHL plates, with worms showing varied degrees of developmental delay.

Treatment	No. of plates	L1s per plate	Mean % survival (min. and max.)	Mean % dauer formation (min. and max.)
Control	11	54.6 ± 3.8	68 (53-81)	0
EHL	12	64.2 ± 7.0	23 (11-40)	24 (0-45)
AuNPs@Citrate	11	58.6 ± 3.2	73 (54-84)	0
AuNPs@EHL	12	48.7 ± 6.6	68 (49-83)	0

In the second set of experiments, using L4 stage worms, there was a small effect on lifetime fecundity in the EHL treated worms, and a delay in reproduction in both the EHL treated and the AuNPs@EHL worms; whilst naked nanoparticles did not obviously affect the L4 stage worms. We can thus conclude and that AuNPs@EHL does have a biological activity. For the treated L4s, there was a difference between treatments in lifetime fecundity (TREATMENT: $F_{3,68} = 2.76$, $p = 0.049$) that is a consequence of a small reduction in lifetime fecundity in the EHL treated worms (EHL treatment significantly different to the control and nanoparticle-treated worms by Fisher's post-hoc testing) (Figure 6, panel A). There is also variation between treatments in early reproduction ($H = 14.22$, $df = 3$, $p = 0.003$), with both the EHL treated and the EHL conjugated nanoparticle treated worms showing a reduced early fecundity ($p < 0.05$ in comparison to control worms via Mann-Whitney test) (Figure 6, panel B).

The L4 assays conducted show that AuNPs@EHL do still retain some activity, suggesting that ingestion in the absence of glyconjugate binding (which is absent in the L1 assay) of the molecule may present a low level of toxicity. The observation that AuNPs@EHL do not agglutinate erythrocytes would suggest that this is a factor. Of course, the inverse hypothesis may also be worthy of investigation, that the toxic A-chain activity may have been altered and that binding still occurs without the cytotoxic effects seen in the intact molecule. As non-RIP lectins have been shown to bind to epithelial cells in the gut causing reduced fitness [36], this requires further study to establish the exact reason for the reduction in toxicity.

Preprints (www.preprints.org) | NOT PEER-REVIEWED | Posted: 9 May 2018 doi:10.20944/preprints201805.0141.v1

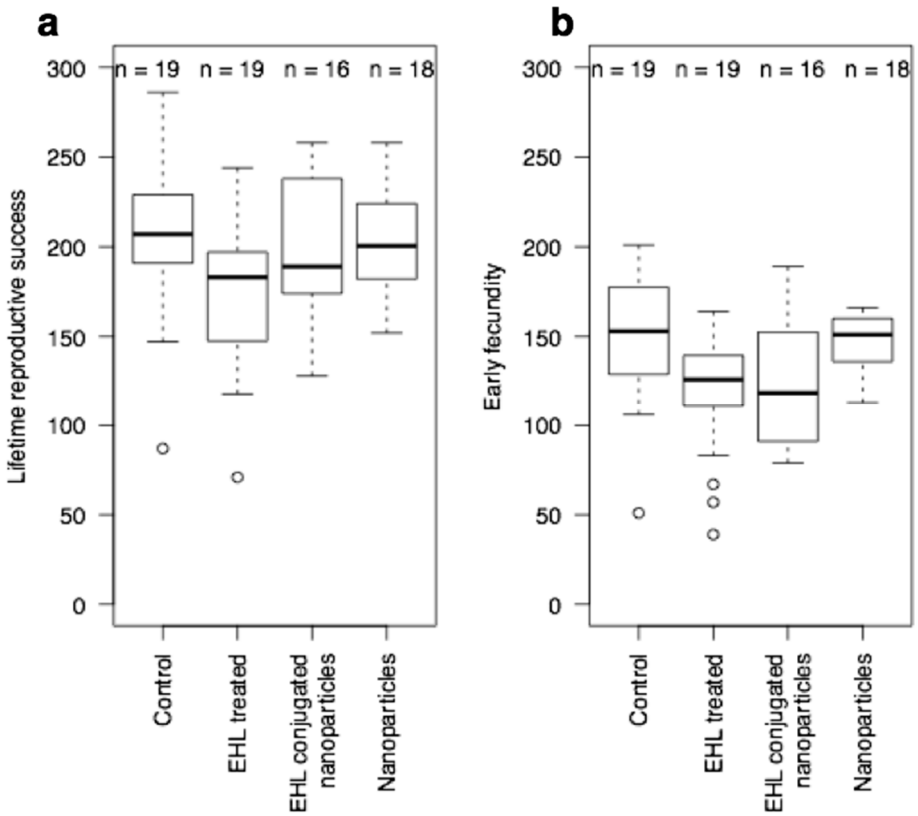

Figure 6. EHL conjugated nanoparticles (AuNPs@EHL) affect early reproduction (early fecundity), but not total reproduction (lifetime reproductive success) of *C. elegans* L4 stage.

4. Conclusion

The synthesis and characterization of gold nanoparticles conjugated with EHL (AuNPs@EHL) was successfully carried out; optimal functionalization was achieved with the addition of 100 µL of EHL (concentration 1090 ± 40 µg/mL) on 5 mL of AuNPs@Citrate ([Au^0] = 0.8 mM). Biological assays on the effect of AuNPs@EHL on *C. elegans* were performed, using first life stage (L1) and pre-adult stage (L4) nematodes, and compared to the effect of naked gold nanoparticles and EHL alone. This preliminary work has shown that the activity of EHL is altered by conjugation and as such resulted in a lessened biological effect towards L1 stage worms. For the assays performed with L4 nematodes, naked nanoparticles do not produce any obvious effect on the worms, while AuNPs@EHL conjugated nanoparticles do produce a similar biological activity to that produced by EHL alone.

Acknowledgments: This work was supported by the Associate Laboratory Research Unit for Green Chemistry - Clean Processes and Technologies - LAQV which is financed by national funds from FCT/MEC (UID/QUI/50006/2013) and co-financed by the ERDF under the PT2020 Partnership Agreement (POCI-01-0145-FEDER - 007265). JFL thanks FCT/MEC (Portugal) for his postdoctoral grant SFRH/BPD/93982/2013. J. D. thanks for her research contract to the research project PTDC/QEQ-MED/2118/2014. J.L.C.; J.F.L; J.D and CL are grateful to the Scientific Society PROTEOMASS (Portugal) for funding support (General Funding Grant). M. T. Mc thanks Canterbury Christ Church University for her doctoral grant. EB and SH are grateful to Canterbury Christ Church University for financial support. H.M.S thanks the IF Research contract by the FCT-MEC Portugal.

Author Contributions: M.-T. Mc conceived, designed and performed the biological experiments, analyzed the data, and contributed to sections of the first draft; J. D. and J.F.L. conceived, designed and performed the experiments related to the synthesis and characterization of the gold functionalized nanoparticles, analyzed the data, and contributed to sections of the first draft; E. B. helped with the conception of the biological experiments, contributed reagents/materials/analysis tools, wrote part of the first draft of the paper, reviewed subsequent drafts, and reviewed the final draft. S. H. conceived and designed the biological experiments, analyzed the data, contributed reagents/materials/analysis tools, and reviewed drafts of the paper. J.L.C. and C. L. analyzed the nanoparticles data, contributed reagents/materials/analysis tools, prepared figures and/or tables, wrote part of the first draft of the paper and reviewed subsequent drafts.

Conflicts of Interest: The authors declare no conflict of interest

References

1. Peumans, W.J.; Van Damme, E. Lectins as plant defense proteins. *Plant Physiology* **1995**, *109*, 347-352. DOI: 10.1104/pp.109.2.347

2. Sharon, N.; Lis, H. History of lectins: From hemagglutinins to biological recognition molecules. *Glycobiology* **2004**, *14*, 53-62. DOI: 10.1093/glycob/cwh122

3. Schubert, M.; Bleuler-Martinez, S.; Butschi, A.; Wälti, M.A.; Egloff P.; Stutz, K.; Yan S.; Wilson, I.B.H.; Hengartner, M.O.; Aebi, M.; Allain, F.H.T.; Künzler, M. Plasticity of the β-trefoil protein fold in the recognition and control of invertebrate predators and parasites by a fungal defence system. *PLoS Pathogens* **2012**, *8:5*, e1002706, DOI: 10.1371/journal.ppat.1002706

4. Delatorre, P.; Rocha, B.A.; Souza, E.P.; Oliveira, T.M.; Bezerra, G.A.; Moreno, F.B.; Azevedo, W.F. Structure of a lectin from Canavalia gladiata seeds: new structural insights for old molecules. *BMC Structural Biology* **2007**, *7*, 52. DOI: 10.1186/1472-6807-7-52

5. Kumar, M.A.; Timm, D.; Neet, K.; Owen, W. Peumans W.J.; Rao, A.G. Characterization of the lectin from the bulbs of Eranthis hyemalis (winter aconite) as an inhibitor of protein synthesis. *Journal of Biological Chemistry* **1993**, *268*, 25176-25183.

6. Rao, K.; Rathore, K.S.; Hodges, T.K.; Fu, X.; Stoger, E.; Sudhakar, D. Bown, D.P. Expression of snowdrop lectin (GNA) in transgenic rice plants confers resistance to rice brown planthopper. *Plant Journal* **1998**, *15*, 469-477, DOI: 10.1046/j.1365-313X.1998.00226.x

7. Peumans, W.J.; Hao, Q.; van Damme, E.J. Ribosome-inactivating proteins from plants: more than RNA N-glycosidases? *The FASEB Journal* **2001**, *15(9)*, 493-1506. DOI: 10.1096/fj.00-0751rev.

8. Edwards, M.G.; Gatehouse, A.M. Biotechnology in crop protection: Towards sustainable insect control. In *Novel biotechnologies for biocontrol agent enhancement and management*, Vurro, M., Gressel, J., Eds; NATO Security through Science Series. Springer: Dordrech, Netherlands, 2007; pp 1-23. ISBN: 978-1-4020-5797-7. DOI: 10.1007/978-1-4020-5799-1_1

9. Cammue, B.P.; Peeters, B.; Peumans, W.J. Isolation and partial characterization of an N-acetylgalactosamine-specific lectin from winter-aconite (*Eranthis hyemalis*) root tubers. *Biochemical Journal* **1985**, *227(3)*, 949-955. DOI: 10.1042/bj2270949

10. George, O.; Solscheid, C.; Bertolo, E.; Lisgarten, D. Extraction and purification of the lectin found in the tubers of *Eranthis hyemalis* (winter aconite). *Journal of Integrated OMICS* **2011**, *1(2)*, 268–272. DOI: 10.5584/jiomics.v1i2.72.

11. McConnell, M.-T., Structural and functional characterisation of Eranthis hyemalis lectin: a type II ribosome inactivating protein. PhD Dissertation. Canterbury Christ Church University, Canterbury UK, 2017.

12. Ju, T.; Otto, V.I.; Cummings, R.D. The Tn antigen—structural simplicity and biological complexity. *Angewandte Chemie International Edition* **2011**, *50(8)*, 1770–1791. DOI: 10.1002/anie.201002313

13. Voss, C.; Eyol, E.; Frank, M.; Von der Lieth, C.W.; Berger, M.R. Identification and characterization of riproximin, a new type II ribosome-inactivating protein with antineoplastic activity from Ximenia americana. *FASEB Journal*, **2006**, *20*, 1194–1196. doi: 10.1096/fj.05-5231fje

14. Bayer, H.; Essig, K.; Stanzel, S.; Frank, M.; Gilderseeve, J.C.; Berger M.R.; Voss, C. Evaluation of Riproximin binding properties reveals a novel mechanism for cellular targeting. *J. of Biol. Chem.* **2012**, *287*, 35873–35886. DOI: 10.1074/jbc.M112.368548

15. Adwan, H.; Bayer, H.; Pervaiz, A.; Sagini, M., Berger, M.R. Riproximin is a recently discovered type II ribosome inactivating protein with potential for treating cancer. *Biotechnology Advances* **2014**, *2(6)*, 1077–1090. DOI: 10.1016/j.biotechadv.2014.03.008

16. McConnell, M.-T.; Lisgarten, D.R.; Byrne, L.J.; Harvey, S.C.; Bertolo, E. Winter Aconite (*Eranthis hyemalis*) Lectin as a cytotoxic effector in the lifecycle of *Caenorhabditis elegans*. *PeerJ* **2015**, 3, e1206. DOI: 10.7717/peerj.1206

17. Boyd, W.A.; Smith, M.V.; Freedman, J.H. *Caenorhabditis elegans* as a model in developmental toxicology. Methods in Molecular Biology **2012**, *889*, 15-24. DOI: 10.1007/978-1-61779-867-2_3

18. Corsi, A.K.; Wightman, B.; Chalfie, M. A Transparent window into biology: A primer on *Caenorhabditis elegans*. *Genetics* **2015**, *200(2)*, 387-407. DOI: 10.1534/genetics.115.176099

19. Cassada, R.C.; Russell, R.L. The dauerlarva, a post-embryonic developmental variant of the nematode *Caenorhabditis elegans*. *Dev. Biol.* **1975**, *46*, 326–342.

20. Hutter, E.; Fendler, J.H. Exploitation of localized surface plasmon resonance. *Advanced Materials* **2004**, *16(19)*, 1685-1706. DOI: 10.1002/adma.200400271

21. Hutter, E.; Maysinger, D. Gold nanoparticles and quantum dots for bioimaging. *Microscopy research and technique* **2011**, *74*(7), 592-604. DOI: 10.1002/jemt.20928

22. Dykman L.; Khlebstov, N. Gold nanoparticles in biomedical applications: recent advances and perspectives. *Chem. Soc. Rev.* **2012**, *41*, 2256-2282. DOI: 10.1039/C1CS15166E

23. Dreaden E.C.; Alkinany, A.M., Huang, X.; Murphy, C.J.; El-Sayed, M.A. The golden age: gold nanoparticles for biomedicine. *Chem. Soc. Rev.* **2012**, *41*, 2740-2779. DOI: 10.1039/C1CS15237H

24. Ahmad, M.Z.; Akhter, S.; Rahman, Z.; Akhter, S.; Anwar, M.; Mallik, N.; Ahmad, F.J. Nanometric gold in cancer nanotechnology: current status and future prospect. *J of Pharmacy and Pharmacology* **2013**, *65(5)*, 634-651. DOI: 10.1111/jphp.12017

25. Kimling, J.; Maier, M.; Okenve, B.; Kotaidis, V.; Ballot, H; Plech, A. Turkevich Method for Gold Nanoparticle Synthesis Revisited. *J. Phys. Chem. B* **2006**, *110 (32)*, 15700–15707. DOI: 10.1021/jp061667w

26. Stiernagle, T. Maintenance of C. elegans. In *WormBook*, The *C. elegans* Research Community, Wormbook, Ed., 2006. DOI: 10.1895/wormbook.1.101.1.

27. Shang, L.; Wang, Y.; Jiang, J.; Dong, S. pH-dependent protein conformational changes in albumin: gold nanoparticle bioconjugates, a spectroscopy study. *Langmuir* **2007**, *23(5)*, 2714–2721. DOI: 10.1021/la062064e

28. De Paoli Lacerda, S. H.; Park, J. J.; Meuse, C.; Pristinski, D.; Becker, M. L.; Karim, a; Douglas, J. F. Interaction of Gold Nanoparticles with Common Human Blood Proteins. *ACS Nano* **2010**, *4*, 365–379. DOI: 10.1021/nn9011187

29. Tsai, D. H.; Delrio, F. W.; Keene, A. M.; Tyner, K. M.; MacCuspie, R. I.; Cho, T. J.; Zachariah, M. R.; Hackley, V. A. Adsorption and Conformation of Serum Albumin Protein on Gold Nanoparticles Investigated Using Dimensional Measurements and in Situ Spectroscopic Methods. *Langmuir* **2011**, *27*, 2464–2477. DOI: 10.1021/la104124d

30. Wang, Y.; Ni, Y. Combination of UV-Vis Spectroscopy and Chemometrics to Understand Protein-Nanomaterial Conjugate: A Case Study on Human Serum Albumin and Gold Nanoparticles. *Talanta* **2014**, *119*, 320–330. DOI: 10.1016/j.talanta.2013.11.026.

31. Hendel, T.; Wuithschick, M.; Kettemann, F.; Birnbaum, A., Rademann, K.; Polte, J. In Situ Determination of Colloidal Gold Concentrations with UV–Vis Spectroscopy: Limitations and Perspectives. *Anal. Chem.* **2014**, *86(22)*, 11115–11124. DOI: 10.1021/ac502053s

32. Scarabelli, L.; Grzelczak, M.; Liz-Marzán. L.M. Tuning Gold Nanorod Synthesis through Prereduction with Salicylic Acid. *Chem. Mater.* **2013**, *25(21)*, pp 4232–4238. DOI: 10.1021/cm402177b

33. Scarabelli, L.; Sánchez-Iglesias, A.; Pérez-Juste, J.; Liz-Marzán. L.M. A "Tips and Tricks" Practical Guide to the Synthesis of Gold Nanorods. *J. Phys. Chem. Lett.* **2015**, *6(21)*, pp 4270–4279. DOI: 10.1021/acs.jpclett.5b02123

34. Wang, P.; Wang, X.; Wang, L.; Hou, X.; Liu, W.; Chen, C. Interaction of gold nanoparticles with proteins and cells. *Sci. and Technol. Adv. Mater*. **2015**, 16(3), 034610. DOI: 10.1088/1468-6996/16/3/034610

35. Thobhani, S.; Attree, S.; Boyd, R.; Kumarswami, N.; Noble, J.; Szymanski, M.; Porter, R. A. Bioconjugation and characterisation of gold colloid-labelled proteins. *Journal of Immunological Methods* **2010**, 356, 60–69. DOI: 10.1016/j.jim.2010.02.007

36. Stutz, K.; Kaech, A.; Aebi, M.; Künzler, M.; Hengartner, M.O. Disruption of the *C. elegans* intestinal brush border by the fungal lectin CCL2 phenocopies dietary lectin toxicity in mammals. *PloS ne* **2015**, *10(6),* e 0129381. DOI: 10.1371/journal.pone.0129381